Rev. Adv. Mater. Tech. vol. 3 no 4 (2021) 29–33
DOI: 10.17586/2687-0568-2021-3-4-29-33

# Structural and Optical Properties of Silver Nanoparticles In Situ Synthesized in ZnO Film by Sol–Gel Method

**L.A. Sokura[1,2], E.A. Ryabkova[1], D.A. Kirilenko[1,2], E.V. Shirshneva-Vaschenko[3]**

[1] ITMO University, Kronverkskiy pr., 49, lit. A, St. Petersburg, 197101, Russia
[2] Ioffe Institute, Politekhnicheskaya str., 26, St Petersburg 194021, Russia
[3] University of Central Florida, 4000 Central Florida Blvd., Orlando, FL 32816, USA

*Received: December 23, 2021*

**Abstract.** We fabricate the samples with two layers of silver nanoparticles embedded in ZnO film exploring sol–gel method by varying the annealing temperatures. The structural properties of the samples are determined by transmission electron microscopy. The effect of the annealing temperature on the nanoparticles plasmon absorption spectra is studied. Annealing at 570 °C results in a shift of the plasmon absorption maximum from 580 nm to 620 nm, due to an increase in the nanoparticles average size from 63 nm to 74 nm. Increasing the annealing temperature to 650 °C results in a shift of plasmon absorption maximum back to 580 nm due to a decrease in the nanoparticles size to 61 nm. Before annealing, the silver nanoparticles of the upper layer locate on top of the nanoparticles of the bottom layer, however, in the plane of the layers, they are arranged randomly at a distance of 30 to 150 nm from each other. As a result of the annealing, the system tended to be ordered, as a result, the nanoparticles in the layers become to be distributed equidistant at 40–70 nm between them; the nanoparticles of the upper layer tend being located between the nanoparticles of the bottom layer.

## 1. INTRODUCTION

Structures with metallic nanoparticles (NPs) in a dielectric or semiconductor matrix have a unique optical property in that electromagnetic radiation results in surface plasmon resonance, which leads to resonant peaks in the absorption spectrum [1]. A local change in the electric field near plasmon NP, among other things, can increase luminescence intensity [2] or absorption efficiency [3], which makes these materials promising for improving the characteristics of various optoelectronic devices.

Structures with plasmon NPs can be produced by chemical deposition, vacuum deposition, ion implantation, or other methods. Most of the methods involve subsequent controlled modification of the structure, that is, a treatment of the material containing metal ions by pulsed laser radiation [4], ultraviolet radiation [5], electron irradiation [6] or high temperatures [7]. Even though many articles have been published on this topic, there does not seem to be any clear physical model of metallic NPs formation in a dielectric matrix. However, NPs are known to be formed as a result of the subsequent addition of metal atoms to each other due to the activation of diffusion processes, whereas the parameters of the resulting NP system are determined by the intensity of external influence and the initial local concentration of metal atoms [4–8].

LEDs, lasers, and similar devices, require NPs to have a diameter from 5 to 100 nm with a narrow size distribution, and also to be ordered in the plane or the volume of the matrix. The concentration or the surface density of NPs, as well as the total thickness of the structure have to be big enough (surface density at least $10^{10}$ cm$^{-2}$, thickness 50 nm and more) to obtain effective absorption of incident radiation. To produce

Corresponding author: L.A. Sokura, e-mail: sokuraliliy@itmo.ru

structures with the given parameters, a formation model of an NP is to be developed, as well as a technology of its manufacturing. However, most of the methods described above have some technological problems. For example, the structures obtained, especially with the thickness of above 50 nm, often have a monotonous decrease in the concentration and the size of NPs within the sample [4]. The sol–gel method used in this paper consists in sequential coating of thin layers of matrix materials and NP metal, which provides a uniform content of metal ions throughout the depth of the matrix without limiting the maximum layer thickness.

The present research is a continuation of studies of optical and structural properties, as well as of the processes of silver nanoparticles formation (Ag NP) in a ZnO semiconductor films using the sol–gel method with high-temperature annealing. In our previous research we have shown that this method provides an ordered Ag NP system within the ZnO film due to Ag diffusion [9]. However, since all previous works were dedicated to the study of ordering in structures with a single NP layer, there is an issue of how the NP formation will occur in structures with more than one NP layer, and whether diffusion will take place between the layers. Thus, the purpose of this paper was to study the Ag diffusion processes occurring in a ZnO film with two NP layers, as well as to determine the effect of the annealing temperature on the morphology and the optical properties of the structures obtained.

## 2. EXPERIMENT

To produce experimental samples the sol–gel method was chosen. In addition to its simplicity and cost efficiency, the sol–gel method has the advantage of providing a homogeneous system of ordered NPs in the layers with a thickness of above 50 nm, which is essential for the challenges faced. The sol–gel method has produced ZnO-based structures with two intermediate layers of Ag NPs.

Polished flat-parallel quartz plates with a thickness of 1 mm and a diameter of 20 mm were used as the substrates for coating. This material was selected because of its high transparency in the visible range of the spectrum and the temperature stability up to 900 °C. Before coating, the substrates were treated with an ultrasonic bath in diluted nitric acid and subsequently with distilled water.

The solution for ZnO layers contained 2-aqueous zinc acetic acid with a concentration of 0.2 M in 2-Methoexyethanol. To stabilize the sol, monoethanolamine was added to the solution in a ratio of 1:1. The solution was stirred on a magnetic stirrer for 60 minutes at a speed of 500 rpm at room temperature, then held for a day for aging and transition to a sol state.

The solution for producing NPs contained silver nitrate in 2-Methoexyethanol with a concentration of 0.05 M. The solution was stirred on a magnetic stirrer for 10 minutes at a speed of 500 rpm at room temperature, no aging was required.

The layers were obtained by a spin-coating method at a speed of 3500 rpm for 10 seconds. After coating, each layer was exposed to air drying for 3 minutes at 300 °C. The structures under study contained two layers of Ag NP: the first 5 layers of ZnO sol were coated followed by the 5 layers of silver nitrate solution, the process was repeated, and 5 more layers of ZnO sol were coated on top. The resulting multilayer structure was annealed in a muffle furnace in the air for 15 minutes at three different temperatures in the range of 570–650 °C. Thus, the obtained series contained a sample after drying at 300 °C (without annealing) and 3 samples sets annealed at temperatures of 570, 600 and 650 °C. The experiments showed that the samples without annealing are purple, and the blue color appeared during the annealing process.

The optical density spectra of the samples were measured using an AvaSpec 2048 fiber-optic spectrometer in the spectral range of 200–1100 nm. The study of the obtained samples structure (the shape, the size and the spatial distribution of NPs) was carried out using a transmission electron microscope (TEM) JEOL JEM-2100F with an accelerating voltage of 200 keV. Thin cross sections of structures with Ag NP in the ZnO film for TEM studies were prepared in accordance with the standard procedure, including initial mechanical thinning and subsequent polishing with an ion beam ($Ar^+$) with an energy of 4 keV [10].

## 3. RESULTS AND DISCUSSION

Figure 1 shows the optical density spectra of obtained structures with two layers of Ag NPs in a ZnO film annealed at different temperatures. Intense absorption at the wavelengths lower than 400 nm corresponds to the edge of the ZnO interband absorption. The optical band gap determined by the spectra was 3.2 eV, which is slightly lower than the reference data for bulk ZnO (3.34–3.37 eV); similar results were reported earlier in Ref. [11].

Absorption bands in the range of 500–700 nm appear to be caused by the surface plasmon resonance in Ag NPs. The NP absorption bands are wide (100 nm and more), they may represent a superposition of the

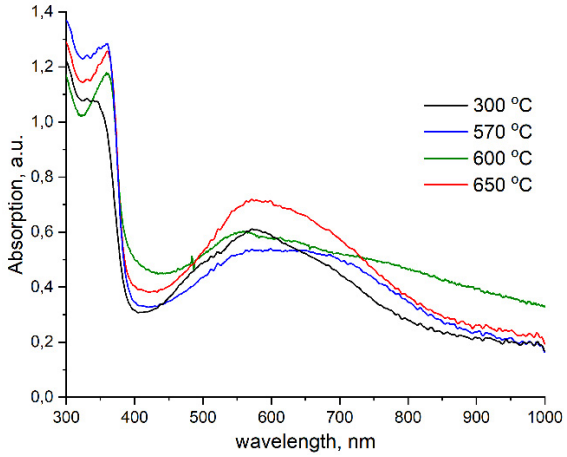


**Fig. 1.** Optical density spectra of the samples with Ag NPs embedded in ZnO films, synthesized by sol–gel method at different annealing temperatures: black line represents samples without annealing (after drying at 300 °C), the blue one corresponds to samples after annealing at 570 °C, the green one – at 600 °C, the red one – at 650 °C.

absorption spectra of the NP ensemble of various sizes. Also, the reason may be the formation of NP with a shape other than spherical, for example, elongated in one or more directions.

The optical density spectra (Fig. 1) show that for a sample annealed at 570 °C, compared with the sample without annealing, subjected only to drying at 300 °C, the intensity of the Ag NP plasmon absorption decreased. Besides, the half-width of the peak increased from 100 nm to 120 nm, and the position of the absorption maximum shifted to the long-wavelength region of the spectrum from 580 nm to 620 nm. In accordance with the Mie theory [12] describing the optical properties of metal NPs, the spectral shift of the plasmon absorption maximum to the long-wavelength region indicates that the average size of NPs in the sample has increased. The size of Ag NP may tend to increase during annealing at a temperature of 570 °C, due to active diffusion. This takes place along with a decrease in their concentration, which is observed on the optical density spectra.

After annealing at the temperatures of 600 °C and 650 °C, the intensity of the NP plasmon absorption peak increased again, and the spectral position of the peak returned to 580 nm, which may indicate the opposite process — a decrease in the NPs size and an increase in their concentration. As stated in Ref. [4], melting of NP metals can occur at temperatures significantly lower than the melting temperature of the bulk material. For silver, the melting point is 960 °C, however, for Ag NP, with a size of 50 nm, it decreases down to 500 °C [13]. Consequently, NP melting may occur in the studied samples during annealing, which leads to a decrease in their size. On the other hand, since the melting point depends on the size of an NP [14], the smaller NPs decrease in size faster than the larger ones, which may result in an increase in the half-width of the absorption peak.

Figure 2 presents TEM cross-sectional images of the samples without annealing and after annealing at the temperatures of 570 and 650 °C for 15 minutes. Analysis of the data given in Fig. 2 confirms that the ZnO film has a polycrystalline structure, the total thickness of all layers makes 170±10 nm and does not change during the annealing. After coating and drying the layers, crystalline grains of ZnO with a size of 5–7 nm are formed, during the annealing process their sizes increase to 20–30 nm. The improvement of the crystalline quality of the ZnO layers, among other factors, was demonstrated by electron diffraction patterns

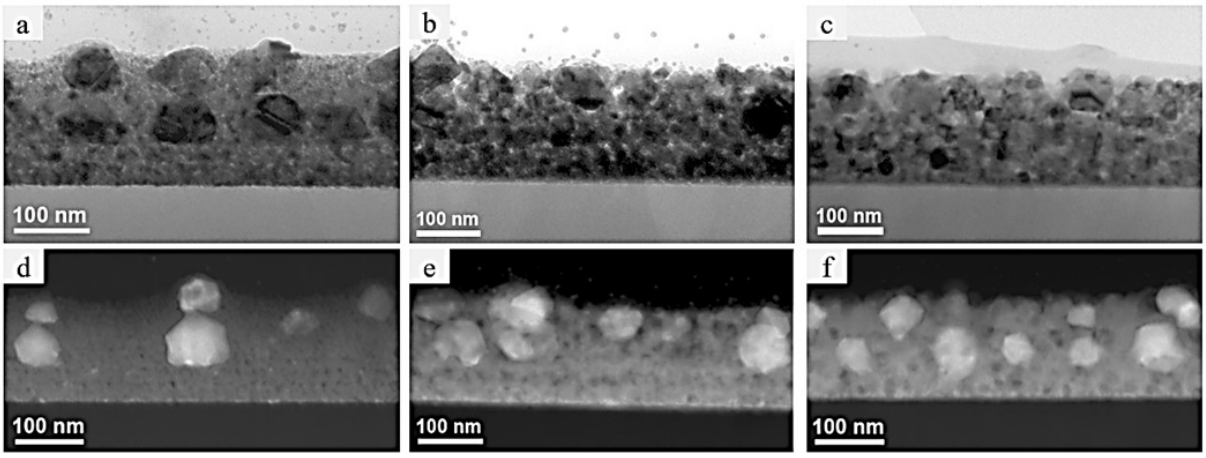


**Fig. 2.** Cross-section TEM (a, b, c) и STEM (d, e, f) images of samples with Ag NP in ZnO film, synthesized by sol–gel method: without annealing (a, d), after annealing at 570 °C (b, e) and at 650 °C (c, f).

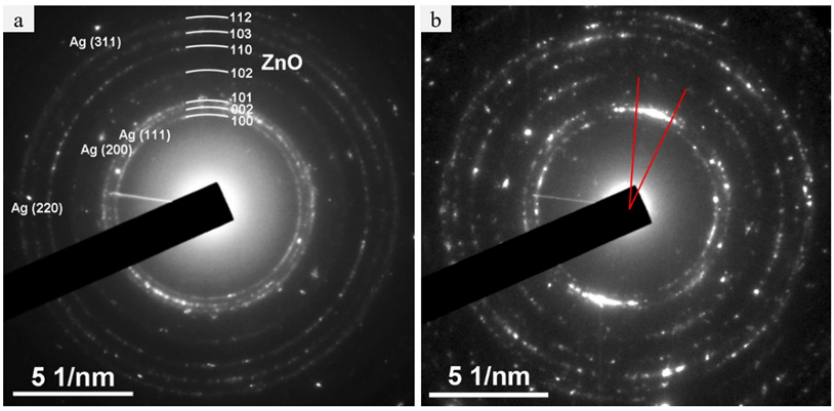


**Fig. 3.** Electron diffraction pattern of samples with Ag NPs in ZnO films, synthesized by sol-gel method: without annealing (a) and after annealing at 570 °C (b).

(Fig. 3), the thickness of polycrystalline rings corresponding to ZnO decreases after annealing, and separate diffraction reflections from ZnO crystallites are observed. Moreover, ZnO crystallites tend to a selected direction for general orientation with a misorientation angle of about 10° (Fig. 3b).

As ZnO crystallized, the image contrast decreased, therefore, the mode of scanning transmission electron microscopy (STEM) was also used for NP studies. This mode has a high contrast when studying materials with a close density (Fig. 2d,e,f). Two layers of Ag NPs parallel to the sample surface were observed on the TEM and STEM cross-sectional images of the samples. NPs were spherical, some had a faceting with a pyramidal or hexagonal shape, common for ZnO nanocrystallites [15].

NPs appeared to be large. Their diameter varied from 50 to 80 nm with an average size of 63 nm even in the sample without annealing. NP dimensions behaved non-linearly with increasing the annealing temperature. The average diameter of NP slightly increased to 74 nm with a spread from 60 to 100 nm after annealing at 570 °C. With a further increase of the annealing temperature to 650 °C, the average diameter of NPs decreased back to 61 nm, but their spread increased significantly from 30 to 90 nm. This behavior of NP sizes was also demonstrated by the above investigation of the optical properties of the samples.

Figure 2 also shows that in the sample without annealing, the NPs are located on top of each other in different layers, forming columns. The distance between the NP columns ranged widely from 30 to 150 nm, the NPs inside the column were located at 5–10 nm from each other. During the annealing, NPs tend to be distributed in layers in a checkerboard manner — the NPs of the upper layer are located between the NPs of the bottom layer. As a result, the distance between them becomes more uniform and ranges from 40 to 70 nm. All geometric parameters obtained for the samples from the TEM are included in Table 1.

## 4. SUMMARY AND CONCLUSIONS

The optical and the structural properties of the samples with two layers of Ag NPs in a ZnO film synthesized by the sol–gel method have been studied. The optical density spectra of the obtained samples contained NP plasmon absorption bands in the range of 500–700 nm. As a result of annealing at 570 °C, a long-wave shift of the plasmon absorption maximum was observed due to an increase in the average NP size from 63 nm to 74 nm. With the annealing temperature increasing to 600–650 °C, the opposite trend has been observed, the maximum of plasmon absorption shifted towards smaller wavelengths, and the NP size decreased to 61 nm.

**Table 1.** Geometric parameters of the samples with the Ag NPs in ZnO films obtained from TEM.

| Size | Without annealing (drying at 300 °C) | Annealing at 570 °C | Annealing at 650 °C |
|---|---|---|---|
| NPs size range, nm | 50–80 | 60–100 | 30–90 |
| Average size of NPs, nm | 63 | 74 | 61 |
| Distance between NPs in layers, nm | 30–150 | 30–90 | 40–70 |
| Distance between NPs layers, nm | 5–10 | 10 | 10–15 |
| Thickness of ZnO layer, nm | 170 | 170–180 | 160–170 |
| ZnO grains size, nm | 5–7 | 15–20 | 20–30 |

The samples obtained did consist of a polycrystalline ZnO film with spherical, pyramidal, or hexagonal Ag NPs. Columns of Ag NPs were formed in the sample without annealing, but they were at a random distance from each other (from 30 to 150 nm). During the annealing, Ag NPs were distributed in the layers in a checkerboard manner, while the distance between them was aligned and made 40–70 nm.

Thus, it has been established that, a system with two Ag NP layers tends to order during annealing, just as one Ag NP layer does. However, in the fabricated samples, the Ag NP size range, and their width of plasmon absorption peak are too high for electronic device applications, which probably requires choosing a more suitable annealing time and/or temperature.

## ACKNOWLEDGEMENTS

The TEM studies were performed using the equipment of the Joint Research Center "Material science and characterization in advanced technology" (Ioffe Institute). The authors are grateful to Prof. A.E. Romanov and Dr. A.M. Smirnov for fruitful discussions.

## REFERENCES

[1] S.A. Maier, *Plasmonics: fundamentals and applications*, Springer, New York, 2007.

[2] N. Bhardwaj, B. Satpati and S. Mohapatra, *Plasmon-enhanced photoluminescence from $SnO_2$ nanostructures decorated with Au nanoparticles*, Applied Surface Science, 2020, vol. 504, art no. 144381. https://doi.org/10.1016/j.apsusc.2019.144381.

[3] A.A. Tabrizi and A. Pahlavan, *Efficiency improvement of a silicon-based thin-film solar cell using plasmonic silver nanoparticles and an antireflective layer*, Optics Communications, 2020, vol. 454, art. no. 124437. https://doi.org/10.1016/j.optcom.2019.124437.

[4] A.L. Stepanov, V.N. Popok, D.E. Hole and A.A. Bukharaev, *Interaction of high-power laser pulses with glasses containing implanted metallic nanoparticles*, Physics of the Solid State, 2001, vol. 43, no. 11, pp. 2192–2198. https://doi.org/10.1134/1.1417202.

[5] M.A. Kudryashov, A.I. Mashin, A.S. Tyurin, A.E. Fedosov, G. Chidichimo and G. De Filpo, *Morphology of a Silver/Polyacrylonitrile Nanocomposite*, Technical Physics, 2011, vol. 56, no. 1, pp. 92–96. https://doi.org/10.1134/S1063784211010154.

[6] A.I. Ignat'ev, A.V. Nashchekin, V.M. Nevedomskii, O.A. Podsvirov, A.I. Sidorov, A.P. Solov'ev and O.A. Usov, *Formation of silver nanoparticles in photothermorefractive glasses during electron irradiation*, Technical Physics, 2011, vol. 56, no. 5, pp. 662–667. https://doi.org/10.1134/S1063784211050148.

[7] I.E. Chentsova, V.I. Dubovik and V.S. Kovivchak, *Synthesis of silver nanoparticles by thermal annealing of thin films*, Herald of Omsk University, 2012, vol. 2, pp. 110–114 (in Russian).

[8] A.V. Red'kov, *Formation of composite materials based on glasses containing a reductant*, Physics of the Solid State, 2012, vol. 54, no. 9, pp. 1875–1881. https://doi.org/10.1134/S1063783412090260.

[9] L.A. Sokura, E.V. Shirshneva-Vaschenko, D.A. Kirilenko, Zh.G. Snezhnaia, P.S. Shirshnev and A.E. Romanov, *Electron-microscopy study of ordered silver nanoparticles synthesized in a ZnO:Al polycrystalline film*, Journal of Physics: Conference Series, 2019, vol. 1410, art. no. 012170. https://doi.org/10.1088/1742-6596/1410/1/012170.

[10] D.S. Rao, K. Muraleedharan, C.J. Humphreys, *TEM specimen preparation techniques*, in: Microscopy: Science, Technology, Applications and Education, ed. by A. Méndez-Vilas and J. Díaz, Formatex, Spain, 2011, pp. 1232–1244.

[11] N.M. Denisov, E.B. Chubenko, V.P. Bondarenko and V.E. Borisenko, *Optical properties of multilayered sol–gel zinc-oxide films*, Semiconductors, 2018, vol. 52, no. 6, pp. 723–728. https://doi.org/10.1134/S1063782618060040.

[12] U. Kreibig and M. Vollmer, *Optical properties of metal clusters*, Springer, Berlin, 1995.

[13] T. Castro, R. Reifenberg, E. Choi and R.P. Andres, *Size-dependent melting temperature of individual nanometer-sized metallic clusters*, Physical Review B, 1990, vol. 42, no. 13, pp. 8548–8556. https://doi.org/10.1103/physrevb.42.8548.

[14] J. Zhu, Q. Fu, Y. Xue and Z.Cui, *Accurate thermodynamic relations of the melting temperature of nanocrystals with different shapes and pure theoretical calculation*, Materials Chemistry and Physics, 2017, vol. 192, no. 1, pp. 22–28. https://doi.org/10.1016/j.matchemphys.2017.01.049.

[15] R.K. Sonker and B.C. Yadav, *Growth mechanism of hexagonal ZnO nanocrystals and their sensing application*, Materials Letters, 2015, vol. 160, pp. 581–584. http://dx.doi.org/10.1016/j.matlet.2015.06.090